LUMINESCENCE PROPERTY OF Sn-DOPED ZnO NANOWIRES BY CURRENT HEATING DEPOSITION

T. JINTAKOSOL[a*], P. SINGJAI[b]
[a]*Department of General Science, Faculty of Science, Srinakharinwirot University, Bangkok 10110, Thailand*
[b]*Department of Physics and Materials Science, Faculty of Science, Chiang Mai University, Chiang Mai 50200, Thailand*

ZnO and Sn doped ZnO nanowires (NWs) were synthesized by current heating deposition. The effect of Sn doped ZnO NWs on their structure and optical characteristics were investigated. ZnO NWs in diameter ranging from 30 to 70 nm and length up to several 10 μm were obtained, whereas that of the Sn-doped ZnO NWs was observed slightly larger, in the range 100-150 nm. Ionoluminescence spectra of ZnO and Sn doped ZnO NWs have showed two emission peaks centered at 386 (UV emission) and 505 nm (green emission). The intensities of green emission increased whereas the intensity of UV emission decreased with increasing Sn content. It is anticipated that increasing intensity of green emission correlates to the density of oxygen vacancy which occurred at the optimum Sn content.

(Received May 6, 2014; Accepted July 2, 2014)

Keywords: Sn-doped ZnO, Nanowires, Luminescence

1. Introduction

One-dimensional (1D) nanostructures of metal oxides have been recently become the subject of extensive research due to their potential application such as functional components for nanoelectronics, optoelectronics and sensing devices [1-5]. ZnO oxide (ZnO) is an exceptionally important material for use in gas sensor [6-9], field emission device [10-11], and luminescence properties [12-15]. The doping of Sn in ZnO is expected to modify the luminescence, structure of ZnO because of the different structure of the electronic shell and the similar size of Sn^{4+} (0.071 nm) and Zn^{2+} (0.074 nm).

Photoluminescence (PL) spectra of materials can provide information of their quality and purity. It is known that visible luminescence of ZnO is due to structural defects, such as oxygen vacancies [16], Zn vacancies and interstitials. Therefore, they normally show visible luminescence properties as observed in PL spectra. Although many researchers synthesized Sn doped ZnO NWs using various techniques such as carbon-assisted synthesis [17] and thermal evaporation process [18].

In this work, ZnO NWs and Sn doped ZnO NWs were synthesized by a current heating deposition. Luminescence properties of the NWs were investigated.

2. Experimental

The ZnO NWs and Sn-doped ZnO NWs were synthesized by a current heating deposition which was recently reported by our group for synthesis of SiC, ZnO and MgO nanowires [19-21].

* Corresponding author: thanut@swu.ac.th

In brief, the raw material was a mixture of 60 wt% Carbon (Sigma-Aldrich, Graphite powder, -325 mesh, >99.99%), 40 wt% ZnO (Sigma-Aldrich, 99.99%) powders. For the growth of Sn-doped ZnO NWs, SnO_2 (Sigma-Aldrich, 99+%) powders at two difference concentration (ZnO:SnO_2, 3:1 and 2:1 wt%) were mixed with ZnO and Carbon powders. The rod was then prepared by adding polyvinyl alcohol (1.5 ml) as a binder, hydraulic die forming at 500 kg to sizes of 12 mm in diameter and 25 mm in length (~ 3.0 g) and drying in an oven at 150 ºC for 3 h. The synthesis was done under flowing argon at a gas flow rate of 2 l/min. To synthesize the NWs, the prepared rod was clipped between two copper electrodes, preheated by a D.C. power supply (Agilent, 6572A) at 40 W (20V, 2A) for 5 min and gradually heated up to about 750-800 ºC (Ultimax infrared thermometer, ux-20P) at 300 W (5V, 60A) for 30 min.

The morphology of the products was characterized by scanning electron microscopy (SEM, JEOL JSM-6335F) and energy dispersive analysis of X-ray (EDX, Oxford). Their crystal structures were analyzed by X-ray diffraction (XRD, Bruker D8 Advance) and transmission electron microscopy (TEM, JEOL JEM-2010), operated at 200 kV. Optical properties were examined by Raman spectroscopy (HORIBA JOBINYVON T 64000) with a 514.5 nm argon ion laser at room temperature and ionoluminescence spectroscopy with excitation energy of 25 keV H^- beam at room temperature (Tandetron accelerator) and Ocean Optics S2000 spectrometer.

3. Results and discussion

The ZnO NWs and Sn-doped ZnO Nws product formed on the rod surface could be seen by naked eye as grey films and easily separated from its core. From the SEM image, as shown in Fig. 1 (a)-(c), a rod-like structure, length up to several tens micrometers of ZnO NWs and Sn-doped ZnO NWs is mainly observed. The diameter of the ZnO NWs is in the range of 30-70 nm, whereas that of the Sn-doped ZnO NWs is slightly larger, in the range 100-150 nm.

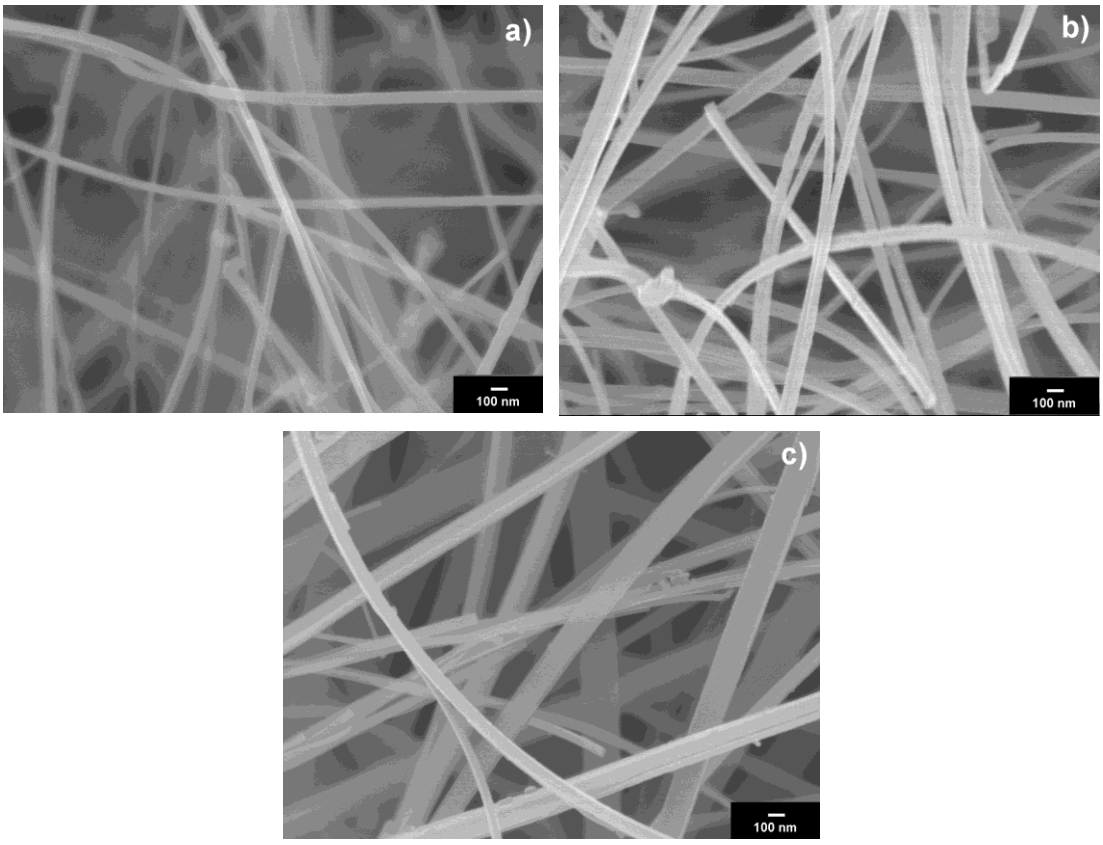

Fig. 1 SEM image of ZnO NWs and Sn doped ZnO NWs.

TEM image and (inset) its corresponding selected area electron diffraction (SAED) pattern of an individual ZnO NWs and Sn-doped ZnO NWs are shown in Fig. 2. These results indicate that the ZnO NWs growth by this present work has a hexagonal structure with (0001) direction along the wires axis (Fig. 2 (a)). This growth directs is in good agreement with the result of several previous reports such as Refs. [22-23]. Fig. 2 (b) shows TEM image of an individual Sn-doped ZnO NWs of ratio 3:1. From Fig. 2 (c), the TEM image of Sn doped ZnO NW of ratio 2:1 show the structure of ZnO has hexagonal structure with a [001] growth direction. This result is similar to some findings in the previous studies [24]. The diameter of a NW is 125 nm, and the thickness of shell layer is 40 nm.

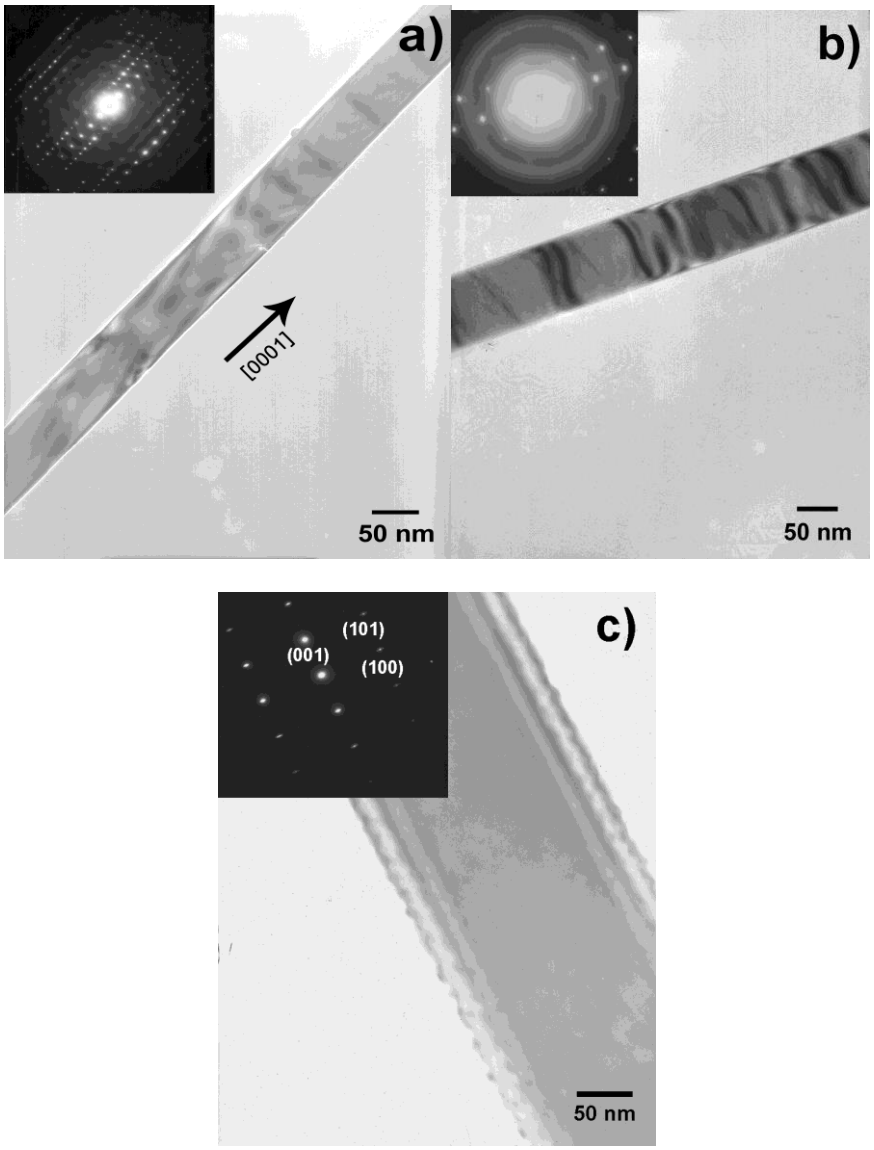

Fig. 2 TEM images of individual nanowires, together with its corresponding SAED pattern (inset), a) ZnO NWs, b) Sn doped ZnO NWs of ratio 3:1 and c) Sn doped ZnO of ratio 2:1.

XRD patterns (Fig. 3) show that the ZnO NWs and Sn-doped ZnO NWs consisted of crystalline ZnO with a hexagonal close-packed structure. The peaks correspond to this structure: (100), (002), (101), (102), (110), (103), (200), (112) and (201) are in good agreement with the JCPDS file number 89-1397 for the wurtzite type with lattice constant a = 3.25 Å and c = 5.20 Å.

Furthermore, Sn phase were detected at (200), (101), (220), (211) and (301) from the Sn-doped ZnO NWs of ratio 3:1 and 2:1 corresponding to Sn tetragonal structure (JCPDS 86-2264) and SnO_2 phase at (110) from 3:1 sample (JCPDS 72-1147).

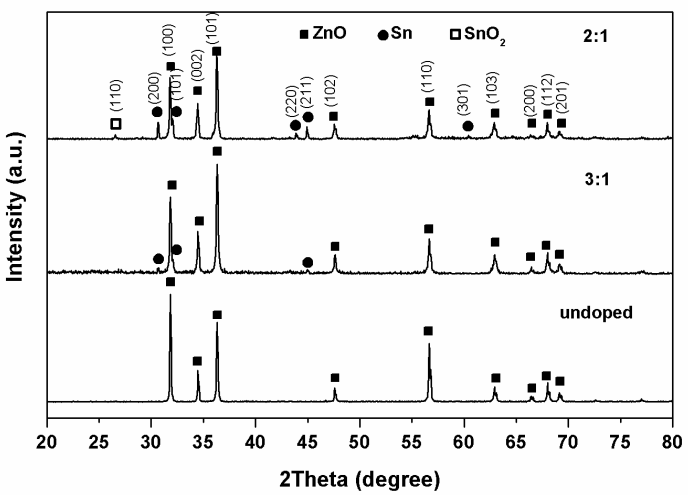

Fig. 3 XRD patterns of the ZnO NWs and Sn doped ZnO NWs.

Raman scattering spectra of ZnO NWs and Sn-doped ZnO NWs are shown in Fig. 4. The peaks could be assigned to active phonon modes which correspond to those of ZnO. The most intense peaks centered at 438 cm^{-1} correspond to E_2 mode, whereas the other peaks, i.e. centered at 334 cm^{-1} correspond to $2E_2$ mode (second order Raman peaks), at 565 cm^{-1} correspond to A_1-LO mode and at 384 cm^{-1} correspond to A_1-TO mode, and at 1149 cm^{-1} correspond to 2LO [25-26]. As reported, the 1LO phonon mode can be attributed to defect-induce mode associate with lattice defects (oxygen vacancies, zinc interstitials or their combination) [20]. A comparison of higher order peaks of 1LO phonon modes is shown in Fig. 4. It can also be seen that the intensity of defect-induce mode frequency for Sn-doped ZnO NWs is higher than that of ZnO NWs, therefore, the peak at 1LO (565 cm^{-1}) may result from the concentration of lattice defect in Sn-doped ZnO NWs become higher with increase of Sn content. In addition, the raman peak at 667 cm^{-1} is correspond to SnO_2 (A_{1g}). In the raman spectrum of the SnO_2, the mode A_{1g} shift toward higher wave number. Katiyar and co-worker [27] reported that the small dimension of the nanowires leads to a downshift of raman peaks, while stress trends to shift raman peak to higher frequency region.

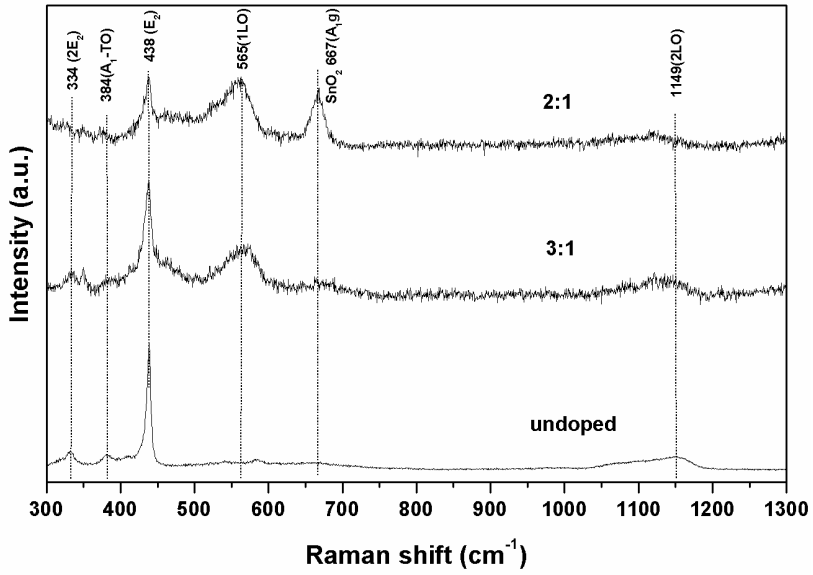

Fig. 4 Raman spectra of the ZnO NWs and Sn doped ZnO NWs.

It is well known that without a catalyst, the growth of ZnO NWs and Sn-doped ZnO NWs is governed by a vapor-solid (VS) process. The growth mechanism NWs can be explained by a carbothermal reduction reaction process [23] or a carbon-assisted synthesis [17]. Similarly, in the case of current heating process, the vapor phases of Zn, Sn and CO are generated by a reduction reaction inside the rod, diffused to the rod surface, and formed the NWs by oxidation reaction.
Fig. 5 shows IL spectra of ZnO NWs and Sn doped ZnO NWs. The spectra from samples have strong green emission center at 505 nm and weak UV emission at 386 nm. The UV peak was observed clearly in the ZnO NWs sample which almost disappeared after increase of Sn content. It is well known that the UV peak arises from free excitonic emission of ZnO. The green emission from ZnO NWs is known as a result of singly ionized oxygen vacancies [28]. Since, the C/ZnO molar ration in this work is as high as ~10 (60:40 wt%), which caused at relative high reductive environment as compared to the previous report [29-31], therefore, high oxygen vacancies in our sample may preferentially occur during the growth.

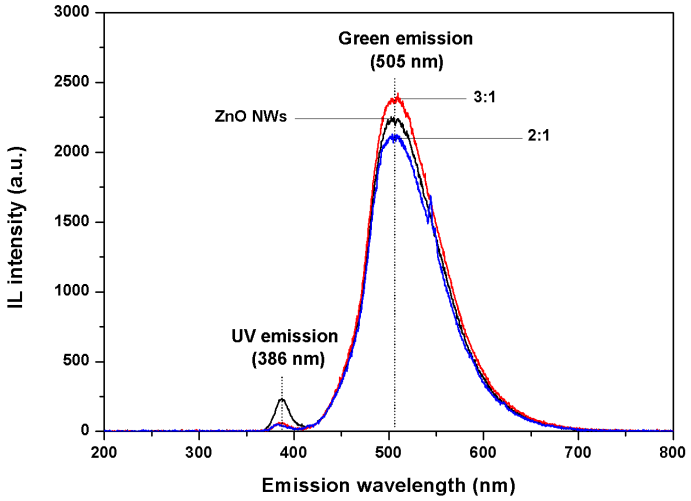

Fig. 5 IL spectra of ZnO NWs and Sn doped ZnO NWs.

Furthermore, the green emission intensity increased with increased Sn content. When Sn goes into substitution position in ZnO lattice were induced share the oxygen with Zn atoms and hence increases the defects of oxygen vacancies, which lead to enhancement of green emission intensity [32]. Seung and co-work [18] reported that the enhancement of green emission of Sn doped ZnO NWs resulted from the largest charge density of Sn will give rise to more defect of oxygen vacancies. The report was in good agreement with our experiment, which the green emission intensity of ratio 3:1 increases with increase of Sn content. However, in the case of ratio 2:1, decrease of green emission intensity might be the result of high oxygen vacancies (Fig. 5). Consequently, a domination of a non-radiation recombination energy transfer process may occur, which corresponded with XRD and Raman results (Fig. 3 and 4) by form SnO_2 phase in sample. Thus, we believed that the green emission intensity correlate to the density of oxygen vacancy which occurred at the optimum Sn content.

4. Conclusions

The ZnO NWs and Sn doped ZnO nanowires were synthesized by current heating deposite. The effect of Sn doped ZnO NWs on their structure and optical characteristics were investigated. The sizes of ZnO NWs are in the range of 30 to 70 nm and length up to several 10 μm. The Sn doped ZnO NWs was observed slightly larger, in the range 100-150 nm. IL spectra indicated that both ZnO NWs and Sn doped ZnO NWs showed strong green emission centered at

505 nm and weak UV emission band centered at 386 nm. The green emission intensity correlate to the density of oxygen vacancy which occurred at the optimum Sn content.

Acknowledgements

This work was supported by the Srinakharinwirot University. The authors would like to thank Ion Beam Analysis Laboratory at Fast Neutron Research Facility, Chiang Mai University.

References

[1] M.H. Huang, S. Mao, H. Feick, H. Yan, Y. Wu, H. Kind, E. Weber, R. Russo, P. Yang, Science **292**, 1897 (2001).
[2] W.I. Park, G.C. Yi, M. Kim, S.J. Pennycook, Adv. Mater. **14**, 1841 (2002).
[3] Z.L. Wang, Mater. Today **7**, 26 (2004).
[4] P.X. Gao, Z.L. Wang, Small **1**, 1 (2005).
[5] H. Yan, R. He, J. Johnson, M. Law, R.J. Saykally, P. Yang, J. Am. Chem. Soc. **125,** 4728 (2003).
[6] J. Xu, Q. Pan, Y. Shun, Z. Tian, Sens. Actuators B **66**, 277 (2000).
[7] X.L. Cheng, H. Zhao, L.H. Huo, S. Gao, J.G. Zhao, Sens. Actuators B **102**, 248 (2004).
[8] C. Xiangfeng, J. Dongli, A.B. Djurišic, Y.H. Leung, Chem. Phys. Lett. **401**, 426 (2005).
[9] Q. Wan, Q.H. Li, Y.J. Chen, T.H. Wang, X.L. He, J.P. Li, C.L. Lin, Appl. Phys. Lett. **84**, 3654 (2004).
[10] C.J. Lee, T.J. Lee, S.C. Lyu, Y. Zhang, H. Ruh, H.J. Lee, Appl. Phys. Lett. **81**, 3648 (2002).
[11] S.H. Jo, J.Y. Lao, Z.F. Ren, R.A. Farrer, T. Baldacchini, J.T. Fourkas, Appl. Phys. Lett. **83**, 4821 (2003).
[12] Y.W. Wang, L.D. Zhang, G.Z. Wang, X.S. Peng, Z.Q. Chu, C.H. Liang, J. Cryst. Growth **234**, 171 (2002).
[13] H. He, Y. Wang, Y. Zou, J. Phys. D: Appl. Phys. **36**, 2972 (2003).
[14] H.S. Kang, J.S. Kang, S.S. Pang, E.S. Shim, S.Y. Lee, Mater. Sci. Eng. B **102**, 313 (2003).
[15] H.S. Kang, J.S. Kang, J.W. Kim, S.Y. Lee, Appl. Phys. Lett. **95**, 1246 (2004).
[16] W. Bai, K. Yu, Q. Zhang, F. Xu, D. Peng, Z. Zhu, Appl. Surf. Sci. **253**, 6835 (2007).
[17] M. Jung, S. Kim, S. Ju, Optic. Mat. **33**, 280 (2011).
[18] S.Y. Bae, C.W. Na, J.H. Kang, J. Park, J. Phys. Chem. B **109**, 2526 (2005).
[19] T. Jintakosol, P. Singjai, Key Eng. Mats. **353-358**, 2171 (2007).
[20] P. Singjai, T. Jintakosol, S. Singkarat, S. Choopun, Mater. Sci. Eng. B **137**, 59 (2007).
[21] T. Jintakosol, P. Singjai, Curr. Appl. Phys. **11**, 1237 (2011).
[22] H.J. Fan, F. Fleischer, W. Lee, K. Nielsch, R. Scholz, M. Zacharias, U. Gösele, A. Dadgar, A. Krost, Superlattices Microstruct. **36**, 95 (2004).
[23] J. Wang, J. Sha, Q. Yang, X. Ma, H. Zhang, J. Yu, D. Yang, Mater. Lett. **59**, 2710 (2005).
[24] Y. Su, L. Li, Y. Chen, Q. Zhou, M. Gao, Q. Chen, Y. Feng, J. Cryst. Growth **311**, 2466 (2009).
[25] K.A. Alim, V.A. Fonoberov, M. Shamsa, A.A. Balandin, J. Appl. Phys. **97**, 124313 (2005).
[26] M. Rajalakshmi, A.K. Arora, B.S. Bendre, S. Mahamuni, J. Appl. Phys. **87**, 2445 (2000).
[27] R.S. Katiyar, P. Dawson, M.M. Hargreave, G.R. Wikinson, J. Phys. C: Solid State Phys. **4**, 2421 (1971).
[28] K. Vanheusden, W.L. Warren, C.H. Seager, D.K. Tallant, J.A. Voigt, B.E. Gnade, J. Appl. Phys. **79**, 7983 (1996).
[29] Y.S. Lim, J.W. Park, S.T. Hong, J. Kim, Mater. Sci. Eng. B, **129**, 100 (2006).
[30] P. Singjai, A. Wongjamras, L.D. Yu, T. Tunkasiri, Chem. Phys. Lett. 366, 51 (2002).
[31] H.J. Fan, F. Fleischer, W. Lee, K. Nielsch, R. Scholz, M. Zacharias, U. Gösele, A. Dadgar, A. Krost, Superlattices Microstruct. **36**, 95(2004).
[32] P.K. Sharma, A.C. Panda, G. Zolnierkiewicz, N. Guskos, C. Rudowicz, J. App. Phys. **106**, 094314 (2009).